Hindawi
Computational and Mathematical Methods
Volume 2022, Article ID 5243466, 11 pages
https://doi.org/10.1155/2022/5243466

Research Article

Approximate Hermite Interpolations for Compactly Supported Linear Canonical Transforms

I. A. Al-Abdi

Department of Mathematics, Faculty of Education and Applied Sciences, Hajjah University, Hajjah, Yemen

Correspondence should be addressed to I. A. Al-Abdi; iqalabdi@gmail.com

Received 15 May 2022; Accepted 18 August 2022; Published 9 September 2022

Academic Editor: Anil Kumar

There has been several Lagrange and Hermite type interpolations of entire functions whose linear canonical transforms have compact supports in $\mathbb{R}$. There interpolation representations are called sampling theorems for band-limited signals in signal analysis. The truncation, amplitude, and jitter errors associated with the Lagrange type interpolations are investigated rigorously. Nevertheless, the amplitude and jitter errors arising from perturbing samples and nodes are not studied before. The aim of this work is to establish rigorous analysis of their types of perturbation errors, which is important from both practical and theoretical points of view. We derive precise estimates for both types of errors and expose various numerical examples.

1. Introduction

In recent times, the interpolation representations in the linear canonical transform (LCT) domain have become one of the important areas in different theoretical and practical disciplines. For instance, it has an important role in signal and image processing [1–4], optics [5–8], filter design [9, 10], radar system analysis [11, 12], and many others (see, e.g., [13, 14]). The LCT of a function $f(z)$ is defined as follows [15–17]:

$$L_f^M(\mathrm{x}) \coloneqq L_f^M[f(z)](x) = \begin{cases} \dfrac{1}{\sqrt{i2\pi b}} \displaystyle\int_{-\infty}^{\infty} f(z) e^{i\left(dz^2 + ax^2 - 2zx\right)/2b} dz, & b \neq 0, \\ \sqrt{d} e^{icdz^2/2} f(dx), & b = 0, \end{cases} \tag{1}$$

where a, b, c, d are real numbers satisfying $ad - cb = 1$. The case $b = 0$, L_f^M is merely a chirp multiplication, and it is excluded. Moreover, we assume that $b > 0$. The importance of the LCT arises from the fact that offers a time-frequency analysis of signals and that it generalizes other important othogonal transformations (see [13] for more details).

Let $\sigma > 0$ be fixed. The space of $L^2(\mathbb{R})$-functions with compact support in the LCT domain is

$$\mathrm{B}_\sigma^2 \coloneqq \left\{ f \in L^2(\mathbb{R}) \colon L_f^M(x) = 0, |x| > \sigma \right\}. \tag{2}$$

It is also called the space of band-limited signals in the LCT domain. If PW_σ^2 denotes the Paley-Wiener space of $L^2(\mathbb{R})$-functions with compact support $[-\sigma, \sigma]$ in the Fourier transform domain, then $f \in \mathrm{B}_\sigma^2$ iff there exists $g \in \mathrm{PW}_{\sigma/b}^2$ such that $f(z) = e^{-i(a/2b)z^2} g(z)$. It is known in this case that $g(z)$ is entire of exponential type σ/b, [18]. Moreover, both B_σ^2 and PW_σ^2 are reproducing kernel Hilbert space, see [18].

The derivation of Lagrange-type and Hermite-type interpolations for elements of B_σ^2 attracts the work of many researchers because of its importance in theoretical and applied problems. If $f \in \mathrm{B}_\sigma^2$, then f has the Lagrange-type sampling representaion:

$$f(z) \coloneqq \sum_{\mathrm{n}=-\infty}^{\infty} \mathrm{e}^{-\mathrm{i}(a/2b)\left(z^2 - z_{\mathrm{n}}^2\right)} f(z_n) S_n(z), z \in \mathbb{R}, \tag{3}$$

where $z_n := n\pi b/\sigma$ and

$$S_n(z) := \text{sinc}\ (\sigma/b(z-z_n)) = \begin{cases} \frac{\sin(\sigma/b(z-z_n))}{\sigma/b(z-z_n)}, & z \neq z_n, \\ 1, & z = z_n, \end{cases} \tag{4}$$

see, e.g., [15, 19–23]. Series (3) converges absolutely on $\mathbb{C}$ and uniformly on compact subsets of $\mathbb{C}$ and on $\mathbb{R}$ (see [24]). The Hermite sampling theorem (or derivative sampling theorem) associated with the LCT is obtained for $f \in B^2_\sigma \subseteq B^2_{2\sigma}$ in [15] (see also [25]) to be

$$f(z) := \sum_{n=-\infty}^{\infty} e^{-i(a/2b)\left(z^2-z_n^2\right)} \cdot \left\{ \left(1 + \frac{ia}{b} z_n(z-z_n)\right) f(z_n) + (z-z_n) f'(z_n) \right\} S_n^2(z), \tag{5}$$

$z \in \mathbb{C}$, $z_n = n\pi b/\sigma$, and $a, b \in \mathbb{R}, b > 0$ are arbitrary. In [26], the authors established a convergence analysis for (5). In particular it is shown that (5) converges absolutely and uniformly on $\mathbb{R}$ and locally uniformly on $\mathbb{C}$. In addition, the truncation error associated with (5) is investigated in both local (pointwise) and global (uniform). For $N \in \mathbb{Z}^+$, $z \in \mathbb{R}$, the truncated series of (5) is

$$f_N^D(z) := \sum_{n=-N}^{N} e^{-i(a/2b)\left(z^2-z_n^2\right)} \cdot \left\{ \left(1 + \frac{ia}{b} z_n(z-z_n)\right) f(z_n) + (z-z_n) f'(z_n) \right\} S_n^2(z), \tag{6}$$

and the associated truncation error is

$$T(N, f; z) := f(z) - f_N^D(z) = \sum_{|n|>N} e^{-i(a/2b)\left(z^2-z_n^2\right)} \cdot \left\{ \left(1 + \frac{ia}{b} z_n(z-z_n)\right) \times f(z_n) + (z-z_n) f'(z_n) \right\} S_n^2(z), \tag{7}$$

For $f \in B^2_\sigma$ and $z^k f(z) \in L^2(\mathbb{R})$, for some $k \in \mathbb{N}$, (7) is estimated in [26] via

$$|T(N, f; z)| \leq \frac{|\sin(\sigma/b)z|^2}{(N+1)^k} \cdot \left\{ \frac{\xi_k E_k}{\sqrt{3}} \times \left(\frac{1}{(N\pi - (\sigma/b)z)^{3/2}} + \frac{1}{(N\pi + (\sigma/b)z)^{3/2}} \right) + \eta_k \left(\frac{1}{\sqrt{N\pi - (\sigma/b)z}} + \frac{1}{\sqrt{N\pi + (\sigma/b)z}} \right) \right\}, \tag{8}$$

where

$$\eta_k := \frac{1}{\sigma\sqrt{\pi}} \left(|a|(N+1)^k \sqrt{\int_N^\infty |zf(z)|^2 dz} + \sqrt{\pi} b\, \xi_k \left[\left(\frac{\sigma}{b}\right) E_k + k E_{k-1} \right] \right), \tag{9}$$

$$E_k := \sqrt{\int_{-\infty}^{\infty} |z^k f(z)|^2 dz}, \xi_k := \frac{(\sigma/b)^{k+1/2}}{\pi^{k+1}\sqrt{(1-4^{-k})}}.$$

In this paper, we will study other types of errors associated with (5). This involves the investigation of rigorous estimates for the amplitude and the jitter errors. This is completed in Sections 2–3. Section 4 is devoted to the numerical examples with illustrative figures and numerical comparisons.

2. Amplitude Error Estimate

This section involves the analysis of the amplitude error associated with the Hermite sampling series with LCT (5). The amplitude error arises from using alternate samples $\tilde{f}(z_n), \widetilde{f'}(z_n)$ instead of the exact ones $f(z_n), f'(z_n)$ in the sampling series (5). Let $\varepsilon_n := f(z_n) - \tilde{f}(z_n)$, $\varepsilon'_n := f'(z_n) - \widetilde{f'}(z_n)$ be uniformly bounded by ε, i.e., $|\varepsilon_n|, |\varepsilon'_n| < \varepsilon$, for a sufficiently small $\varepsilon > 0$. The amplitude error is defined for $z \in \mathbb{R}$ in this case to be

$$A(\varepsilon, f; z) := \sum_{n=-\infty}^{\infty} e^{-i(a/2b)\left(z^2-z_n^2\right)} \cdot \left\{ \left(1 + \frac{ia}{b} z_n(z-z_n)\right) \varepsilon_n + (z-z_n)\varepsilon'_n \right\} S_n^2(z), \tag{10}$$

where the following decay conditions are presumed

$$|\varepsilon_n| \leq |f(z_n)|, |\varepsilon'_n| \leq |f'(z_n)|, n \in \mathbb{Z}. \tag{11}$$

For $f \in B^2_\sigma$, we define $\|f\|_\infty := \sup_{z\in R}|f(z)|$.

Theorem 1. *Suppose that $f \in B^2_\sigma$ satisfies a decay condition*

$$|f(z)| \leq \frac{A}{|z|^{\alpha+1}}, z \neq 0, \tag{12}$$

where $A > 0$ and $1/2 < \alpha \leq 1$ are constants, and let (11) holds. Then, for

$$0 < \varepsilon \leq \min\left\{ \frac{\pi b}{\sigma}, \frac{\sigma}{\pi b}, \frac{1}{\sqrt{e}} \right\}, \tag{13}$$

we have

$$\|A(\varepsilon, f; z)\|_\infty \le \frac{4e^{1/4}}{\sigma(\alpha+1)}\Big\{\sqrt{3}\,e(\sigma+b)+\rho(\varepsilon^{-10}) + \sqrt{2}\,|a|\left(\frac{\sigma}{\pi b}\right)^3 \varepsilon^{-1/\alpha+1} + \frac{2\pi b^2}{\sigma} M_1 \rho(\varepsilon^{-10}) + \sqrt{2}\,|a|\left(\frac{\pi b}{\sigma}\right)^3 M_2\Big\}\varepsilon \log\left(\frac{1}{\varepsilon}\right), \tag{14}$$

where

$$M_1 := \frac{3\sigma}{\pi b}\left(|f(0)| + A\left(\frac{\sigma}{\pi b}\right)^{\alpha+1}\right), M_2 := A\left(\frac{\sigma}{\pi b}\right)^{\alpha+2},$$
$$\rho(x) := \frac{2\sigma A}{\pi}\left(\rho(2x) + \frac{\pi}{\sqrt{2}} + 2\right), \rho(x) := \gamma + \log(x), \tag{15}$$

and γ is the Euler-Mascheroni constant.

Proof. Let $z \in \mathbb{R}$. From the triangle inequality and using the fact that $|e^{i\theta}| = 1, \theta \in \mathbb{R}$, we obtain

$$\begin{aligned}|A(\varepsilon, f; z)| &= \left|\sum_{n=-\infty}^{\infty} e^{-i(a/2b)(z^2-z_n^2)}\left\{\left(1+\frac{ia}{b}z_n(z-z_n)\right)\varepsilon_n + (z-z_n)\varepsilon'_n\right\}S_n^2(z)\right| \\ &\le \sum_{n=-\infty}^{\infty}\left|\left\{\left(1+\frac{ia}{b}z_n(z-z_n)\right)\varepsilon_n + (z-z_n)\varepsilon'_n\right\}S_n^2(z)\right| \\ &\le \sum_{n=-\infty}^{\infty}\left|\varepsilon_n S_n^2(z)\right| + \sum_{n=-\infty}^{\infty}\left|\frac{a}{b}z_n(z-z_n)\varepsilon_n S_n^2(z)\right| + \sum_{n=-\infty}^{\infty}\left|(z-z_n)\varepsilon'_n S_n^2(z)\right|.\end{aligned} \tag{16}$$

From (4) we have

$$|A(\varepsilon, f; z)| \le \sum_{n=-\infty}^{\infty}\left|\varepsilon_n S_n^2(z)\right| + \frac{|a|}{\sigma}\sum_{n=-\infty}^{\infty}\left|z_n\varepsilon_n \sin\left(\frac{\sigma}{b}(z-z_n)\right)S_n(z)\right| + \frac{b}{\sigma}\sum_{n=-\infty}^{\infty}\left|\varepsilon'_n \sin\left(\frac{\sigma}{b}(z-z_n)\right)S_n(z)\right|. \tag{17}$$

Now let $p, q > 1$ be such that $(1/p) + (1/q) = 1$. Applying Hölder's inequality and using the fact that $|S_n(z)| \le 1$ leads to

$$|A(\varepsilon, f; z)| \le \left\{\left(\sum_{n=-\infty}^{\infty}|\varepsilon_n|^p\right)^{1/p} + \frac{|a|}{\sigma}\left(\sum_{n=-\infty}^{\infty}|z_n\varepsilon_n|^p\right)^{1/p} + \frac{b}{\sigma}\left(\sum_{n=-\infty}^{\infty}|\varepsilon'_n|^p\right)^{1/p}\right\}\left(\sum_{n=-\infty}^{\infty}|S_n(z)|^q\right)^{1/q}. \tag{18}$$

Substituting from the inequality (see [18]),

$$\left(\sum_{n=-\infty}^{\infty}|S_n(z)|^q\right)^{1/q} < p \tag{19}$$

in (18) yields

$$|A(\varepsilon, f; z)| \le p\left\{\left(\sum_{n=-\infty}^{\infty}|\varepsilon_n|^p\right)^{1/p} + \frac{|a|}{\sigma}\left(\sum_{n=-\infty}^{\infty}|z_n\varepsilon_n|^p\right)^{1/p} + \frac{b}{\sigma}\left(\sum_{n=-\infty}^{\infty}|\varepsilon'_n|^p\right)^{1/p}\right\}. \tag{20}$$

Now, we estimate the infinite sums above. Applying Minkowski's inequality, we obtain for $N \ge 1$

$$\left(\sum_{n=-\infty}^{\infty}|\varepsilon_n|^p\right)^{1/p} \le \left(\sum_{|n|\le N}|\varepsilon_n|^p\right)^{1/p} + \left(\sum_{|n|>N}|\varepsilon_n|^p\right)^{1/p} \tag{21}$$

also

$$\left(\sum_{n=-\infty}^{\infty}|z_n\varepsilon_n|^p\right)^{1/p} \le \left(\sum_{|n|\le N}|z_n\varepsilon_n|^p\right)^{1/p} + \left(\sum_{|n|>N}|z_n\varepsilon_n|^p\right)^{1/p}. \tag{22}$$

For $p \ge 2$ such that $\alpha p \ge 2$, we get from (11) and (12)

$$\begin{aligned}\left(\sum_{|n|>N}|\varepsilon_n|^p\right)^{1/p} &\le \left(\sum_{|n|>N}\left|f\left(\frac{n\pi b}{\sigma}\right)\right|^p\right)^{1/p} \\ &\le A\left(\frac{\sigma}{\pi b}\right)^{\alpha+1}\left(\sum_{|n|>N}\frac{1}{|n|^{p\alpha+p}}\right)^{1/p} \\ &= A\left(\frac{\sigma}{\pi b}\right)^{\alpha+1}\left(2\sum_{n>N}\frac{1}{n^{p\alpha+p}}\right)^{1/p} \\ &\le A\left(\frac{\sigma}{\pi b}\right)^{\alpha+1}\left(2\int_N^{\infty}\frac{1}{z^{p\alpha+p}}dz\right)^{1/p} \\ &\le M_2\left(\frac{\pi b}{\sigma}\right)\left(\frac{2}{p\alpha+p-1}\right)^{1/p}\frac{1}{N^{\alpha+1-1/p}}.\end{aligned} \tag{23}$$

Similarly,

$$\left(\sum_{|n|>N}|z_n\varepsilon_n|^p\right)^{1/p} \le \left(\sum_{|n|>N}\left|\left(\frac{n\pi b}{\sigma}\right)f\left(\frac{n\pi b}{\sigma}\right)\right|^p\right)^{1/p} \le M_2\left(\frac{\pi b}{\sigma}\right)^2\left(\frac{2}{p\alpha-1}\right)^{1/p}\frac{1}{N^{\alpha-1/p}}. \tag{24}$$

Moreover,

$$\left(\sum_{n=-N}^{N}|\varepsilon_n|^p\right)^{1/p} \le \varepsilon(2N+1)^{1/p}, \tag{25}$$

and

$$\left(\sum_{n=-N}^{N}|z_n\varepsilon_n|^p\right)^{1/p} \le 2^{1/p}\left(\frac{\pi b}{\sigma}\right)\varepsilon N^{1+1/p}. \tag{26}$$

Combining (23) and (25), as well as (24) and (26), we get for $N\ge 1, p\ge 2$

$$\left(\sum_{n=-\infty}^{\infty}|\varepsilon_n|^p\right)^{1/p} \le \varepsilon(2N+1)^{1/p} + M_2\left(\frac{\pi b}{\sigma}\right)\left(\frac{2}{p\alpha+p-1}\right)^{1/p} \times \frac{1}{N^{\alpha+1-(1/p)}}, \tag{27}$$

and

$$\left(\sum_{n=-\infty}^{\infty}|z_n\varepsilon_n|^p\right)^{1/p} \le 2^{1/p}\left(\frac{\pi b}{\sigma}\right)\varepsilon N^{1+1/p} + M_2\left(\frac{\pi b}{\sigma}\right)^2\left(\frac{2}{p\alpha-1}\right)^{1/p} \times \frac{1}{N^{\alpha-1/p}}. \tag{28}$$

Since $f(t)$ satisfies Condition (12), then from (11) and Minkowski's inequality, we obtain for $N\ge 1, p\ge 2$:

$$\left(\sum_{|n|>N}|\varepsilon_n'|^p\right)^{1/p} < \left(\sum_{|n|>N}\left|f'\left(\frac{n\pi b}{\sigma}\right)\right|^p\right)^{1/p} < \left(\sum_{n>N}\left|f'\left(\frac{n\pi b}{\sigma}\right)\right|^p\right)^{1/p} + \left(\sum_{-n>N}\left|f'\left(\frac{n\pi b}{\sigma}\right)\right|^p\right)^{1/p}. \tag{29}$$

We have as follows (see [27]):

$$\left(\sum_{\pm n>N}\left|f'\left(\frac{n\pi b}{\sigma}\right)\right|^p\right)^{1/p} < \frac{M_1\rho(N^2)}{N^{1-1/p}} + \frac{M_2(\rho(2N^2)+2)}{N^{\alpha+1-(1/p)}}. \tag{30}$$

Hence,

$$\left(\sum_{|n|>N}|\varepsilon_n'|^p\right)^{1/p} < \frac{2M_1\rho(N^2)}{N^{1-1/p}} + \frac{2M_2(\rho(2N^2)+2)}{N^{\alpha+1-(1/p)}}. \tag{31}$$

Furthermore,

$$\left(\sum_{n=-N}^{N}|\varepsilon_n'|^p\right)^{1/p} \le \varepsilon(2N+1)^{1/p}, \tag{32}$$

Combining (31) and (32), we get for $N\ge 1, p\ge 2$

$$\left(\sum_{n=-\infty}^{\infty}|\varepsilon_n'|^p\right)^{1/p} \le \varepsilon(2N+1)^{1/p} + \frac{2M_1\rho(N^2)}{N^{1-(1/p)}} + \frac{2M_2(\rho(2N^2)+2)}{N^{\alpha+1-(1/p)}}, \tag{33}$$

Substituting from (27), (28), and (33) into (20), we get

$$|A(\varepsilon,f;z)| \le p\left\{\varepsilon\left(1+\frac{b}{\sigma}\right)(2N+1)^{1/p} + 2^{1/p}\left(\frac{|a|\pi b}{\sigma^2}\right)\varepsilon N^{1+1/p} + \frac{2bM_1\rho(N^2)}{\sigma N^{1-1/p}} + \left(\frac{\pi b}{\sigma}\right)^2\left(\frac{2}{p\alpha-1}\right)^{1/p}\frac{|a|M_2}{\sigma N^{\alpha-1/p}} + \frac{bM_2}{\sigma N^{\alpha+1-1/p}}\left(2\rho(2N^2) + \pi\left(\frac{2}{p\alpha+p-1}\right)^{1/p} + 4\right)\right\}. \tag{34}$$

When $\sigma \ge \pi b$, we choose N and p to be

$$N = \varepsilon^{-1/\alpha+1}\left(\frac{\sigma}{\pi b}\right)^{(\alpha+1)p/(\alpha+1)p-1}, p = \frac{4}{(\alpha+1)}\log\left(\frac{1}{\varepsilon}\right). \tag{35}$$

Since $\varepsilon \le \{(\pi b/\sigma), (1/\sqrt{e})\}$, then $(\sigma/\pi b) \le (1/\varepsilon)$ and $N\ge 1$. By simple calculations, we have

$$(2N+1)^{1/p} \le \sqrt{3}\,e^{5/4}, N^{1+1/p} \le e^{1/4}\varepsilon^{-1/\alpha+1}\left(\frac{\sigma}{\pi b}\right)^4,$$

$$N^{1/p-1} \le e^{1/4}\varepsilon\frac{\pi b}{\sigma}, N^{1/p-(\alpha+1)} \le e^{1/4}\varepsilon\left(\frac{\pi b}{\sigma}\right)^{(\alpha+1)},$$

$$N^{1/p-\alpha} \le e^{1/4}\varepsilon\frac{\pi b}{\sigma}, \left(\frac{2}{p\alpha+p-1}\right)^{1/p} \le \sqrt{2},$$

$$\left(\frac{2}{p\alpha-1}\right)^{1/p} \le \sqrt{2}, \rho(N^2) \le \gamma + 10\log\left(\frac{1}{\varepsilon}\right). \tag{36}$$

Combining (34), (36) and noting that $p=(4/(\alpha+1))\log(1/\varepsilon)$, we obtain (14). If $0<\sigma<\pi b$, we take $N=\lfloor \varepsilon^{-(1/(\alpha+1))}(\pi b/\sigma)^{(((\alpha+1)p)/((\alpha+1)p-1))}\rfloor$, and by the same manner, we can prove (14). □

3. Jitter Error Estimate

In this section, we will derive the jitter error estimate associated with (5) which arises when the sampling nodes $n\pi b/\sigma, n\in\mathbb{Z}$ are perturbed from the exact nodes. Let δ_n, $\delta'_n, n\in\mathbb{Z}$ denote the sets of perturbation values. For a sufficiently small $\delta>0$ and $|\delta_n|, |\delta'_n|\le\delta$, $n\in\mathbb{Z}$, the jitter error $J(\delta,f;z)$ associated with (5) is defined for $z\in\mathbb{R}$ by

$$J(\delta,f;z):=\sum_{n=-\infty}^{\infty}e^{i(a/2b)(z_n^2-z^2)}\left\{\left(1+\frac{ia}{b}z_n(z-z_n)\right)\times(f(z_n)-f(z_n+\delta_n))+(z-z_n)\left(f'(z_n)-f'\left(z_n+\delta'_n\right)\right)\right\}S_n^2(z). \tag{37}$$

In the following, we derive estimate for the jitter error according to the decay Condition (12).

Theorem 2. *Let $f\in B_\sigma^2$ be such that Condition (12) holds. Then for*

$$0<\delta\le\min\left\{\frac{\pi b}{\sigma},\frac{\sigma}{\pi b},\frac{1}{\sqrt{e}}\right\}, \tag{38}$$

we have

$$\|J(\delta,f;z)\|_\infty\le\frac{4e^{1/4}}{\sigma(\alpha+1)}\left\{C_1\|f'\|_\infty+\sqrt{3}be\|f''\|_\infty+\frac{4\pi b^2M_1\rho(\delta^{-10})}{\sigma}+2\sqrt{2}\,|a|M_2\left(\frac{\pi b}{\sigma}\right)^3+2\rho\left(\delta^{-10}\right)\right\}\delta\log\left(\frac{1}{\delta}\right), \tag{39}$$

where

$$C_1:=\sqrt{5}\,\sigma e^{3/4}+\sqrt{2}|a|\delta^{-1/\alpha+1}\left(\frac{\sigma}{\pi b}\right)^3, \tag{40}$$

$M_1, M_2, \rho(x)$, and $\rho(x)$ are defined in (15).

Proof. Let $p,q>1$ such that $(1/p)+(1/q)=1$. Appling the triangle inequality to (37) and using (4) yield

$$\begin{aligned}|J(\delta,f;z)|\le&\sum_{n=-\infty}^{\infty}\left|(f(z_n)-f(z_n+\delta_n))S_n^2(z)\right|\\&+\frac{|a|}{\sigma}\sum_{n=-\infty}^{\infty}\left(|z_n(f(z_n)-f(z_n+\delta_n))|\times\left|\sin\left(\frac{\sigma}{b}(z-z_n)\right)S_n(z)\right|\right)\\&+\frac{b}{\sigma}\sum_{n=-\infty}^{\infty}\left(\left|\left(f'(z_n)-f'\left(z_n+\delta'_n\right)\right)\right|\times\left|\sin\left(\frac{\sigma}{b}(z-z_n)\right)S_n(z)\right|\right).\end{aligned} \tag{41}$$

From Hölder's inequality (19) and using the fact that $|S_n(z)|\le1, z\in\mathbb{R}$, we obtain

$$\begin{aligned}|J(\delta,f;z)|\le p\Bigg\{&\left(\sum_{n=-\infty}^{\infty}|\{f(z_n)-f(z_n+\delta_n)\}|^p\right)^{1/p}+\frac{|a|}{\sigma}\left(\sum_{n=-\infty}^{\infty}|z_n\{f(z_n)-f(z_n+\delta_n)\}|^p\right)^{1/p}\\&+\frac{b}{\sigma}\left(\sum_{n=-\infty}^{\infty}\left|\left\{f'(z_n)-f'\left(z_n+\delta'_n\right)\right\}\right|^p\right)^{1/p}\Bigg\}.\end{aligned} \tag{42}$$

From Annaby and Asharabi [27], we have

$$\left(\sum_{n=-\infty}^{\infty}|\{f(z_n)-f(z_n+\delta_n)\}|^p\right)^{1/p}\le\sqrt{5}e\delta\|f'\|_\infty+2\sqrt{2}A\delta e^{1/4}, \tag{43}$$

and

$$\left(\sum_{n=-\infty}^{\infty}\left|\left\{f'(z_n)-f'\left(z_n+\delta'_n\right)\right\}\right|^p\right)^{1/p}\le\delta\|f''\|_\infty(2N+1)^{1/p}+\frac{4M_1\,\rho(N^2)}{N^{1-1/p}}+\frac{4M_2\left(\rho(2N^2)+2\right)}{N^{\alpha+1-1/p}}. \tag{44}$$

It remains to estimate

$$\left(\sum_{n=-\infty}^{\infty}|z_n\{f(z_n)-f(z_n+\delta_n)\}|^p\right)^{1/p}. \tag{45}$$

For convenience, let

$$h(z_n):=|z_n\{f(z_n)-f(z_n+\delta_n)\}|^p. \tag{46}$$

Using the mean value theorem, $N \geq 1$ leads to

$$\begin{aligned}\left(\sum_{|n|\leq N} h(z_n)\right)^{1/p} &= \left(\sum_{|n|\leq N} \left|z_n f'(s_n)\delta_n\right|^p\right)^{1/p} \\ &\leq \delta \left\|f'\right\|_\infty \left(\sum_{|n|\leq N} \left|\frac{n\pi b}{\sigma}\right|^p\right)^{1/p} \\ &= \delta \frac{\pi b}{\sigma} \left\|f'\right\|_\infty \left(2\sum_{n=1}^{N} n^p\right)^{1/p} \\ &\leq 2^{1/p}\delta \frac{\pi b}{\sigma}\left\|f'\right\|_\infty N^{1+1/p},\end{aligned} \tag{47}$$

where $s_n \in [(n\pi b/\sigma), (n\pi b/\sigma) + \delta_n]$, $|n| \leq N$. Applying Minkowski's inequality yields

$$\begin{aligned}\left(\sum_{|n|>N} h(z_n)\right)^{1/p} \leq &\left(\sum_{|n|>N} |z_n f(z_n)|^p\right)^{1/p} \\ &+ \left(\sum_{|n|>N} |z_n f(z_n+\delta_n)|^p\right)^{1/p}.\end{aligned} \tag{48}$$

Using (12), and choosing $p \geq 2$ such that $\alpha p \geq 2$ leads to

$$\begin{aligned}\left(\sum_{|n|>N} |(z_n) f(z_n)|^p\right)^{1/p} &\leq A\left(\frac{\sigma}{\pi b}\right)^{\alpha} \left(\sum_{|n|>N} \frac{1}{|n|^{p\alpha}}\right)^{1/p} \\ &= A\left(\frac{\sigma}{\pi b}\right)^{\alpha}\left(2\sum_{n>N}\frac{1}{n^{p\alpha}}\right)^{1/p} \\ &\leq \left(\frac{\sigma}{\pi b}\right)^{\alpha}\left(2\int_N^\infty \frac{1}{z^{p\alpha}}dz\right)^{1/p} \\ &= M_2\left(\frac{\pi b}{\sigma}\right)^2\left(\frac{2}{p\alpha-1}\right)^{1/p} \times \frac{1}{N^{\alpha-1/p}}.\end{aligned} \tag{49}$$

Hence,

$$\begin{aligned}\left(\sum_{|n|>N} h(z_n)\right)^{1/p} \leq &\left(\sum_{|n|>N} |z_n f(z_n)|^p\right)^{1/p} \\ &+ \left(\sum_{|n|>N} |z_n f(z_n+\delta_n)|^p\right)^{1/p} \\ \leq &\, 2M_2\left(\frac{\pi b}{\sigma}\right)^2\left(\frac{2}{p\alpha-1}\right)^{1/p}\frac{1}{N^{\alpha-(1/p)}},\end{aligned} \tag{50}$$

Table 1: Comparison between $f_N^C(\cdot)$ and $f_N^D(\cdot)$ where $N = 10; 20; 30$ of Example 3.

z_i	N	$\left\|f(z_i) - f_N^C(z_i)\right\|$	$\left\|f(z_i) - f_N^D(z_i)\right\|$
0.25	10	1.16332×10^{-4}	4.16650×10^{-5}
	20	1.56681×10^{-5}	2.90720×10^{-6}
	30	4.75966×10^{-6}	5.94953×10^{-7}
0.75	10	3.52826×10^{-4}	4.28018×10^{-5}
	20	4.71388×10^{-5}	2.92797×10^{-6}
	30	1.42974×10^{-5}	5.96872×10^{-7}
1.25	10	6.01323×10^{-4}	4.52465×10^{-5}
	20	7.90176×10^{-5}	2.97029×10^{-6}
	30	2.38908×10^{-5}	6.00743×10^{-7}
1.75	10	8.71706×10^{-4}	4.94052×10^{-5}
	20	1.11592×10^{-4}	3.03586×10^{-6}
	30	3.35778×10^{-5}	6.06634×10^{-7}
2.25	10	1.17736×10^{-3}	5.60931×10^{-5}
	20	1.45176×10^{-4}	3.12734×10^{-6}
	30	4.33978×10^{-5}	6.14651×10^{-7}

where we have used the same calculations as in (49) to estimate the second sum of (48). Substituting from (43)–(47) and (50) into (42) yields

$$\begin{aligned}|J(\delta, f; z)| \leq p\Bigg(&\sqrt{5}e\delta\left\|f'\right\|_\infty + 2\sqrt{2}A\delta e^{1/4} \\ &+ \frac{2^{1/p}|a|\pi b\delta}{\sigma^2}\left\|f'\right\|_\infty N^{1+1/p} \\ &+ \frac{b\delta}{\sigma}\left\|f''\right\|_\infty (2N+1)^{1/p} \\ &+ \frac{2|a|M_2}{\sigma}\left(\frac{\pi b}{\sigma}\right)^2\left(\frac{2}{p\alpha-1}\right)^{1/p}\frac{1}{N^{\alpha-(1/p)}} \\ &+ \frac{4bM_1\rho(N^2)}{\sigma N^{1-(1/p)}} + \frac{4bM_2\left(\rho(2N^2)+2\right)}{\sigma N^{\alpha+1-(1/p)}}\Bigg).\end{aligned} \tag{51}$$

When $\sigma \geq \pi b$, we choose N and p to be

$$N = \delta^{-1/\alpha+1}\left(\frac{\sigma}{\pi b}\right)^{(\alpha+1)p/(\alpha+1)p-1}, p = \frac{4}{(\alpha+1)} \log\left(\frac{1}{\delta}\right). \tag{52}$$

Hence, as in (36), we get

$$\begin{aligned}&(2N+1)^{1/p} \leq \sqrt{3}\,e^{5/4}, N^{1/p-(\alpha+1)} \leq e^{1/4}\delta\left(\frac{\pi b}{\sigma}\right)^{(\alpha+1)}, \\ &N^{1/p-1} \leq e^{1/4}\delta\frac{\pi b}{\sigma}, N^{1+1/p} \leq e^{1/4}\delta^{-1/\alpha+1}\left(\frac{\sigma}{\pi b}\right)^4,\end{aligned}$$

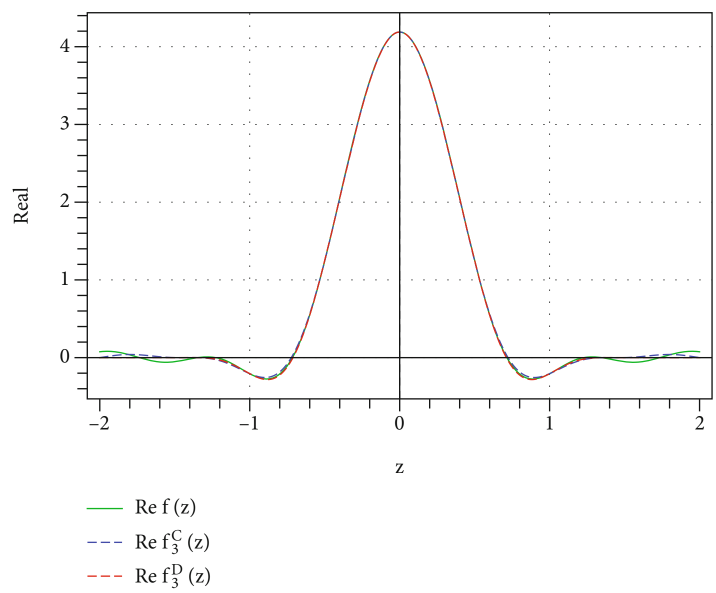

(a)

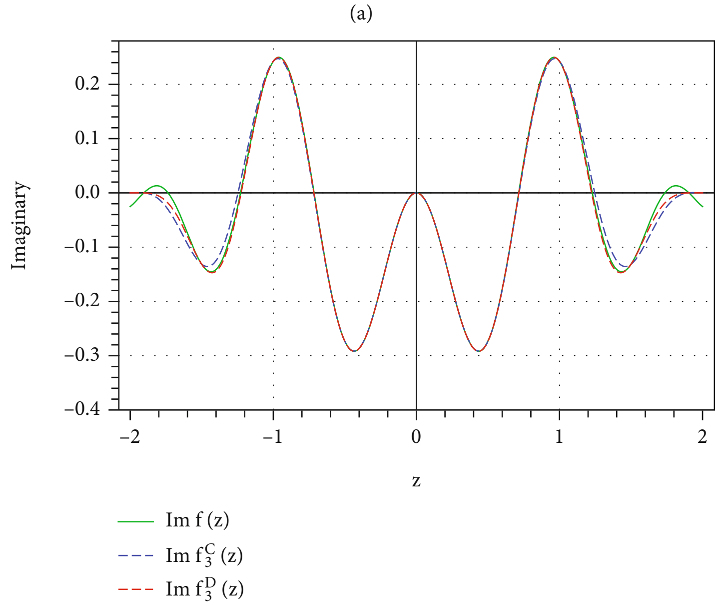

(b)

Figure 1: Illustrations associated with Example 3. (a) The green continuous line is a real part of $f(z)$, while the blue and the red dashed lines are real parts of $f_3^C(z)$ and $f_3^D(z)$, respectively. (b) The green continuous line is an imaginary part of $f(z)$, while the blue and the red dashed lines are imaginary parts of $f_3^C(z)$ and $f_3^D(z)$, respectively.

$$N^{1/p-\alpha} \le e^{1/4}\delta\frac{\pi b}{\sigma}, \rho\left(N^2\right) \le \gamma + 10\log\left(\frac{1}{\delta}\right), \quad \left(\frac{2}{p\alpha - 1}\right)^{1/p} \le \sqrt{2}. \tag{53}$$

Substituting from (53) into (51) and noting $p = (4/(\alpha + 1))\log(1/\delta)$, we obtain (39). When $0 < \sigma < \pi b$, take $N = \lfloor \delta^{-(1/(\alpha+1))}(\pi b/\sigma)^{(((\alpha+1)p)/((\alpha+1)p-1))} \rfloor$, and proceed as in the previous case. □

4. Numerical Examples

This section contains three examples. The first example shows that the use of the Hermite sampling theorem with LCT (5) in approximation theory may be better compared to the classical sampling theorem with LCT (3). In the other two examples, we give tables illustrating the amplitude and jitter errors for some numerical values where $\mathscr{B}(N, f; z)$, $\mathscr{A}(\varepsilon, f; z)$, and $\mathscr{J}(\delta, f; z)$ denote to the bound of the truncation error in (8), the bound of the amplitude error in (14), and the bound of jitter error in (39), respectively. For

Table 2: Exact error $|f(z) - f_{\varepsilon,20}(z)|$ and its bound $\mathscr{B}(20, f; z) + \mathscr{A}(\varepsilon, f; z)$ of Example 4.

z_i	$\varepsilon = 6 \times 10^{-6}$ Absolute error	Bound	$\varepsilon = 4 \times 10^{-6}$ Absolute error	Bound	$\varepsilon = 2 \times 10^{-6}$ Absolute error	Bound
0.6	9.10196×10^{-6}	5.39522×10^{-3}	6.06823×10^{-6}	3.89367×10^{-3}	3.0345×10^{-6}	2.27246×10^{-3}
1.2	1.13933×10^{-5}	6.00578×10^{-3}	7.59643×10^{-6}	4.50424×10^{-3}	3.79955×10^{-6}	2.88303×10^{-3}
1.8	1.27884×10^{-5}	6.70498×10^{-3}	8.52717×10^{-6}	5.20343×10^{-3}	4.26597×10^{-6}	3.58222×10^{-3}
2.4	1.29357×10^{-5}	7.17046×10^{-3}	8.62586×10^{-6}	5.66891×10^{-3}	4.31603×10^{-6}	4.0477×10^{-3}
3.0	1.17621×10^{-5}	7.18759×10^{-3}	7.84351×10^{-6}	5.68605×10^{-3}	3.92497×10^{-6}	4.06484×10^{-3}

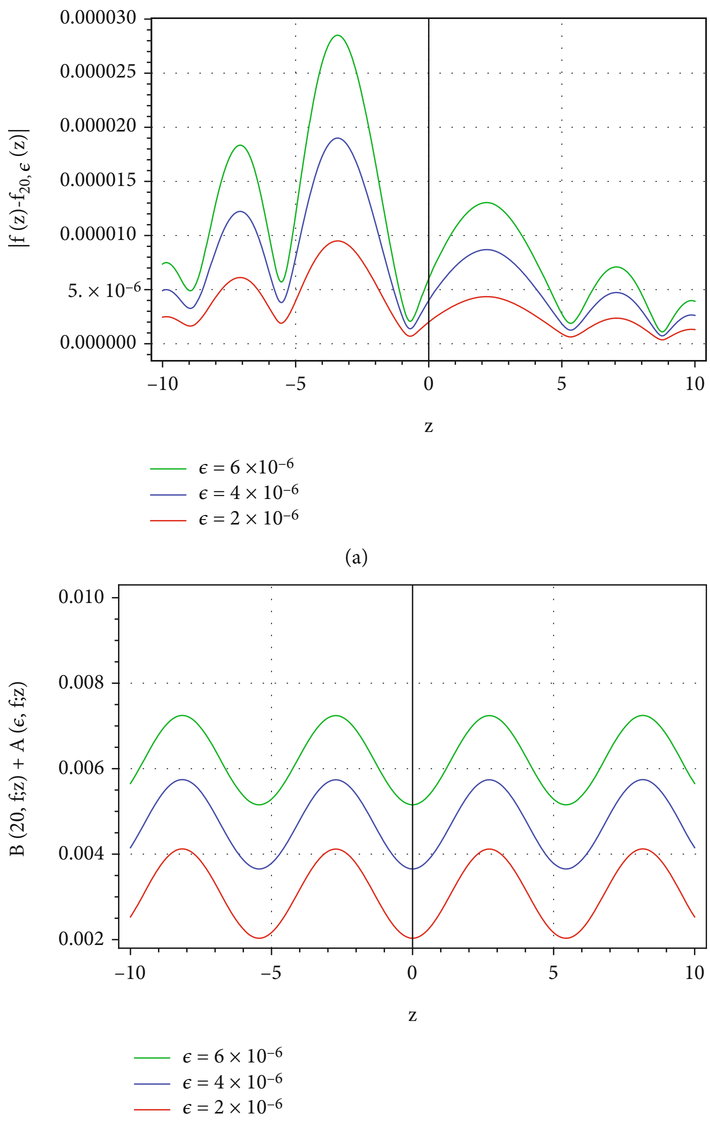

Figure 2: Figures for $|f(z) - f_{\varepsilon,20}(z)|$ (a), $\mathscr{B}(20, f; z) + \mathscr{A}(\varepsilon, f; z)$ (b), where $z \in [-10, 10]$ and $\varepsilon = 6 \times 10^{-6}, 4 \times 10^{-6}, 2 \times 10^{-6}$, respectively.

Table 3: Exact error $|f(z) - f_{20}(\delta; z)|$ and its bound $\mathscr{B}(20, f; z) + \mathscr{J}(\delta, f; z)$ of Example 5.

z_i	$\delta = 9 \times 10^{-8}$ Absolute error	Bound	$\delta = 6 \times 10^{-8}$ Absolute error	Bound	$\delta = 3 \times 10^{-8}$ Absolute error	Bound
0.6	2.87792×10^{-9}	5.29278×10^{-4}	1.97282×10^{-9}	3.95763×10^{-4}	1.07791×10^{-9}	2.45933×10^{-4}
1.2	1.52818×10^{-9}	5.18661×10^{-4}	1.03765×10^{-9}	3.85145×10^{-4}	5.47544×10^{-10}	2.35315×10^{-4}
1.8	7.99524×10^{-10}	5.23896×10^{-4}	5.79877×10^{-10}	3.90381×10^{-4}	3.66721×10^{-10}	2.40551×10^{-4}
2.4	4.75446×10^{-10}	5.25238×10^{-4}	3.6769×10^{-10}	3.91723×10^{-4}	2.74189×10^{-10}	2.41893×10^{-4}
3.0	8.57322×10^{-11}	5.17634×10^{-4}	6.85318×10^{-11}	3.84118×10^{-4}	5.40306×10^{-11}	2.34288×10^{-5}

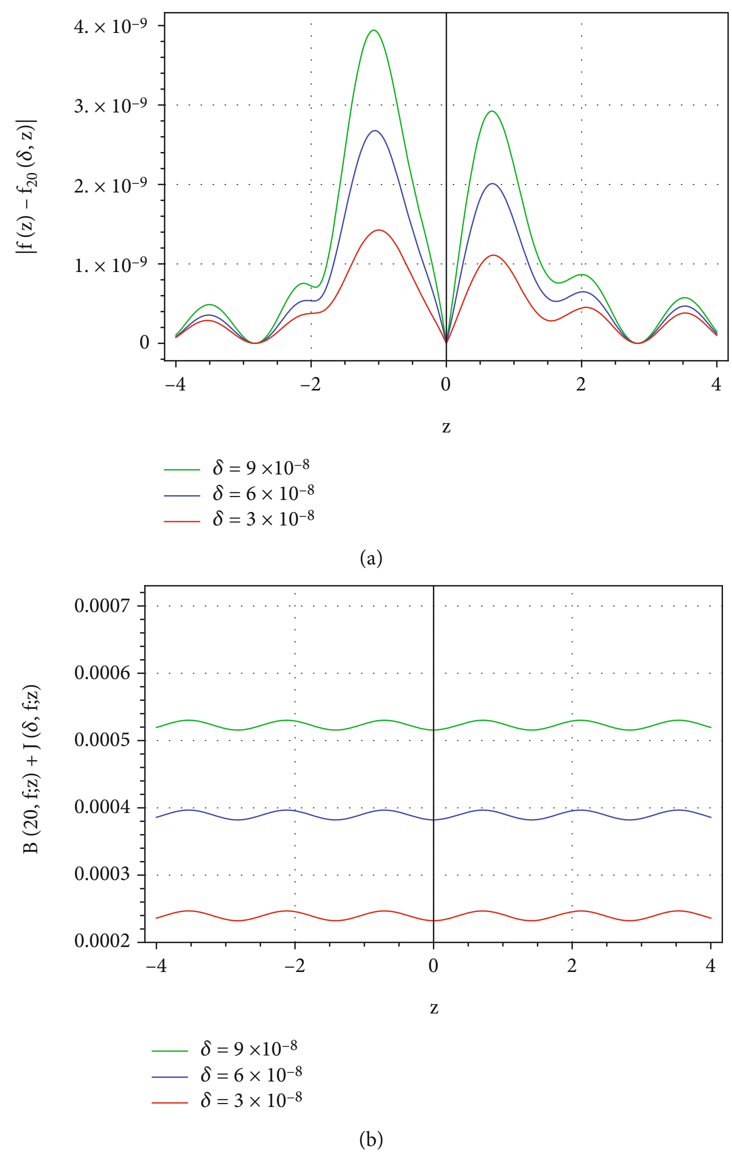

Figure 3: Illustrations associated with Example 5. $|f(z) - f_{20}(\delta, z)|$ (a) and $\mathscr{B}(20, f; z) + \mathscr{J}(\delta, f; z)$ (b), where $z \in [-4, 4]$ and $\delta = 9 \times 10^{-8}$, 6×10^{-8}, 3×10^{-8}, respectively.

$f \in B_\sigma^2$, $z \in \mathbb{R}$ and $N \in \mathbb{N}$, we set

$$f_N^C(z) := \sum_{n=-N}^{N} e^{-ia/2b\left(z^2-Z_n^2\right)} f(z_n) S_n(z),$$
$$\left|f(z) - f_{\varepsilon,N}^D(z)\right| = \left| f(z) - \sum_{|n|\le N} \left\{ e^{ia/2b\left(z_n^2-z^2\right)} \times \left(\left(1 + \left(\frac{ia}{b}\right) z_n (z-z_n)\right) \tilde{f}(z_n) + (z-z_n)\tilde{f}'(z_n) \right) S_n(z) \right\} \right| \le \mathscr{B}(N, f; z) + \mathscr{A}(\varepsilon, f; z),$$
$$\left|f(z) - f_N^D(\delta, z)\right| = \left| f(z) - \sum_{|n|\le N} \left\{ e^{ia/2b\left(z_n^2-z^2\right)} \times \left\{ (1 + (ia/b) z_n (z-z_n)) f(z_n+\delta_n) + (z-z_n) f'\left(z_n + \delta_n'\right) \right\} S_n(z) \right\} \right| \le \mathscr{B}(N, f; z) + \mathscr{J}(\delta, f; z). \tag{54}$$

Example 3. The function

$$f(z) = \frac{e^{-i\left(z^2/2\right)} \sin\left(\sqrt{2}\pi z\right)}{\pi^2 (2z - z^3)}. \tag{55}$$

is a $B_\pi^2 \subseteq B_{2\pi}^2$ function where $a = b = d = (1/\sqrt{2})$. Table 1 demonstrates the comparison between the reconstruction of f using the classical technique $f_N^C(z)$ and the Hermite interpolations $f_N^D(z)$ when $N = 10,20,30$. As Table 1 indicates, the absolute errors decrease as N increases for both techniques. Moreover, the Hermite interpolation approximations are superior to the classical sampling representation of f. Figure 1 illustrates comparison between $f(z), f_N^C(z)$ and $f_N^D(z)$ when $|z| \le 2, N = 3$.

Example 4. Consider the $B_{1/2}^2$-function

$$f(z) = \frac{e^{-i\left(z^2/\left(2\sqrt{3}\right)\right)} \left(\sqrt{3} z \cos\left(\left(z/\sqrt{3}\right)\right) - 3 \sin\left(\left(z/\sqrt{3}\right)\right)\right)}{2\pi^2 z^3}. \tag{56}$$

Here, we take $a = d = 1/2, b = \sqrt{3}/2$. Table 2 and Figure 2 show the comparison between absolute error $|f(z) - f_{\varepsilon,N}(z)|$ and its bound $\mathscr{B}(N, f; z) + \mathscr{A}(\varepsilon, f; z)$ where $N = 20$ and $\varepsilon = 6 \times 10^{-6}, 4 \times 10^{-6}, 2 \times 10^{-6}$, respectively, as well as the effect of ε on the amplitude error. We notice that the error bounds are quite realistic. Moreover, as predicted by the theory, the precision increases when ε decreases.

Example 5. In this example, we consider the function

$$f(z) = e^{-iz^2/2} \left(\frac{\cos\left(\pi z/\sqrt{2}\right) - 1}{\pi^2 z^2} \right)^2 \in B_{\pi/2}^2. \tag{57}$$

Table 3 and Figure 3 exhibit the absolute jitter error $|f(z) - f_N(\delta; z)|$ and its associated bound $\mathscr{B}(N, f; z) + \mathscr{J}(\delta, f; z)$ with $a = b = d = 1/\sqrt{2}$, $N = 20$ and, $\delta = 9 \times 10^{-8}$, $6 \times 10^{-8}, 3 \times 10^{-8}$, respectively, as well as the effect of δ on the jitter error. It can be seen that as δ decreases, accuracy improves.

5. Conclusions

In this paper, we investigated the error analysis of the Hermite sampling theorem associated with the linear canonical transform (LCT). We provided estimates for both amplitude and jitter errors when alternative samples and nodes are implemented, respectively. The study fills a gap in the error analysis associated with Hermite sampling representation for entire functions of exponential type.

Data Availability

No data were used to support this study.

Conflicts of Interest

The author has no conflict of interest for this submission.

References

[1] Z.-J. Huang, S. Cheng, L.-H. Gonga, and N.-R. Zhou, "Nonlinear optical multi-image encryption scheme with two-dimensional linear canonical transform," *Optics and Lasers in Engineering*, vol. 124, article 105821, 2020.

[2] Y. Guo and B.-Z. Li, "Blind image watermarking method based on linear canonical wavelet transform and QR decomposition," *IET Image Processing*, vol. 10, no. 10, pp. 773–786, 2016.

[3] H. Sharma and N. Khatri, "A novel colour image encryption algorithm based on linear canonical transform," in *2017 International Conference on Nascent Technologies in Engineering (ICNTE)*, pp. 1–5, Navi Mumbai, January 2017.

[4] Y. Su, C. Tang, B. Li, and Z. Lei, "Optical colour image watermarking based on phase-truncated linear canonical transform and image decomposition," *Journal of Optics*, vol. 20, no. 5, article 055702, 2018.

[5] T. Alieva, M. J. Bastiaans, and M. L. Calvo, "Fractional transforms in optical information processing," *EURASIP Journal on Advances in Signal Processing*, vol. 2005, no. 10, pp. 1498–1519, 2005.

[6] T. Alieva and M. J. Bastiaans, "Phase-space rotations and orbital stokes parameters," *Optics Letters*, vol. 34, no. 4, pp. 410–412, 2009.

[7] T. Alieva, J. A. Rodrigo, A. Cámara, and M. J. Bastiaans, "The linear canonical transformations in classical optics," in *Linear Canonical Transforms*, pp. 113–178, Springer, New York, NY, 2016.

[8] M. A. Kutay, H. M. Ozaktas, and J. A. Rodrigo, "Optical implementation of linear canonical transforms," in *Linear Canonical Transforms*, pp. 179–194, Springer, New York, 2016.

[9] B. Barshan, M. A. Kutay, and H. M. Ozalctas, "Optimal filtering with linear canonical transformations," *Optics Communication*, vol. 135, no. 1-3, pp. 32–36, 1997.

[10] J. Shi, X. Liu, X. Fang, X. Sha, W. Xiang, and Q. Zhang, "Linear canonical matched filter: theory, design, and applications," *IEEE Transactions on Signal Processing*, vol. 66, no. 24, pp. 6404–6417, 2018.

[11] M. J. Hackert, "Explanation of launch condition choice for GRIN multimode fiber attenuation and bandwidth measurements," *Journal of Lightwave Technology*, vol. 10, no. 2, pp. 125–129, 1992.

[12] X. Huang, L. Zhang, S. Li, and Y. Zhao, "Radar high speed small target detection based on keystone transform and linear canonical transform," *Digital Signal Processing*, vol. 82, pp. 203–215, 2018.

[13] J. J. Healy, M. A. Kutay, H. M. Ozaktas, and J. T. Sheridan, *Linear canonical transforms: Theory and applications*, Springer, New York, NY, USA, 2016.

[14] R. Tao, L. Qi, and Y. Wang, *Theory and Applications of the Fractional Fourier Transform, Beijing*, Tsinghua Univ. Press, China, 2004.

[15] B.-Z. Li, R. Tao, and Y. Wang, "New sampling formulae related to linear canonical transform," *Signal Processing*, vol. 87, no. 5, pp. 983–990, 2007.

[16] M. Moshinsky and C. Quesne, "Linear canonical transformations and their unitary representations," *Journal of Mathematical Physics*, vol. 12, no. 8, pp. 1772–1780, 1971.

[17] H. M. Ozaktas, Z. Zalevsky, and M. A. Kutay, *The Fractional Fourier Transform with Applications in Optics and Signal Processing*, Wiley, New York, 2001.

[18] J. R. Higgins, *Sampling Theory in Fourier and Signal Analysis Foundations*, Oxford University Press, Oxford, 1996.

[19] H. M. Ozaktas and D. Mendlovic, "Fractional Fourier optics," *JOSA A*, vol. 12, no. 4, pp. 743–751, 1995.

[20] H. M. Ozaktas and D. Mendlovic, "Fourier transforms of fractional order and their optical interpretation," *Optics Communication*, vol. 101, no. 3-4, pp. 163–169, 1993.

[21] A. Stern, "Sampling of linear canonical transformed signals," *Signal Processing*, vol. 86, no. 7, pp. 1421–1425, 2006.

[22] R. Tao, B.-Z. Li, Y. Wang, and G. K. Aggrey, "On sampling of band-limited signals associated with the linear canonical transform," *IEEE Transactions on Signal Processing*, vol. 56, pp. 5454–5464, 2008.

[23] X. Xia, "On bandlimited signals with fractional Fourier transform," *IEEE Signal Processing Letters*, vol. 3, no. 3, pp. 72–74, 1996.

[24] M. H. Annaby and R. M. Asharabi, "Error estimates associated with sampling series of the linear canonical transforms," *IMA Journal of Numerical Analysis*, vol. 35, no. 2, pp. 931–946, 2015.

[25] Y. Liu, K. Kou, and I. Ho, "New sampling formulae for non-bandlimited signals associated with linear canonical transform and non linear Fourier atoms," *Signal Processing*, vol. 90, no. 3, pp. 933–945, 2010.

[26] M. H. Annaby, I. A. Al-Abdi, A. F. Ghaleb, and M. S. Abou-Dina, *Hermite interpolation theorems for band-limited functions of the linear canonical transforms with equidistant samples*.

[27] M. H. Annaby and R. M. Asharabi, "Error analysis associated with uniform Hermite interpolations of bandlimited functions," *Journal of the Korean Mathematical Society*, vol. 47, no. 6, pp. 1299–1316, 2010.